AD_____

Award Number: W81XWH-05-1-0002

TITLE: Computational Study of Cytolytic Peptides: Monomeric-Oligomeric Structures and Ligand Interactions

PRINCIPAL INVESTIGATOR: Buyong Ma, Ph.D.
Ruth Nussinov, Ph.D.

CONTRACTING ORGANIZATION: SAIC Frederick, Inc.
Frederick, MD 21702-1201

REPORT DATE: November 2005

TYPE OF REPORT: Annual

PREPARED FOR: U.S. Army Medical Research and Materiel Command
Fort Detrick, Maryland 21702-5012

REPORT DOCUMENTATION PAGE

Form Approved
OMB No. 0704-0188

1. REPORT DATE *(DD-MM-YYYY)*	**2. REPORT TYPE**	**3. DATES COVERED** *(From - To)*
01-11-2005	Annual	25 Oct 2004 – 24 Oct 2005

4. TITLE AND SUBTITLE
Computational Study of Cytolytic Peptides: Monomeric-Oligomeric Structures and Ligand Interactions

5a. CONTRACT NUMBER

5b. GRANT NUMBER
W81XWH-05-1-0002

5c. PROGRAM ELEMENT NUMBER

6. AUTHOR(S)
Buyong Ma, Ph.D.
Ruth Nussinov, Ph.D.

E-mail: mab@ncifcrf.gov

5d. PROJECT NUMBER

5e. TASK NUMBER

5f. WORK UNIT NUMBER

7. PERFORMING ORGANIZATION NAME(S) AND ADDRESS(ES)
SAIC Frederick, Inc.
Frederick, MD 21702-1201

8. PERFORMING ORGANIZATION REPORT NUMBER

9. SPONSORING / MONITORING AGENCY NAME(S) AND ADDRESS(ES)
U.S. Army Medical Research and Materiel Command
Fort Detrick, Maryland 21702-5012

10. SPONSOR/MONITOR'S ACRONYM(S)

11. SPONSOR/MONITOR'S REPORT NUMBER(S)

12. DISTRIBUTION / AVAILABILITY STATEMENT
Approved for Public Release; Distribution Unlimited

13. SUPPLEMENTARY NOTES

14. ABSTRACT
We have mostly followed our initial plan described in the Statement of Work to investigate membrane disrupting peptide dynamics and membrane interactions. In the first year of research, we have focused on two systems (Protegrin-1, β−Defensin). The major progresses have been made in PG-1 membrane interactions, and the β−defensin oligomerization also has preceded well. The important scientific finding during the research period is the elucidation of peptide membrane thinning mechanism. We observed that local thinning of lipid bilayers mediated by the peptide is enhanced in the lipid bilayer containing POPG, consistent with experimental results of selective membrane targeting. The conformational dynamics of Protegrin-1, especially the highly charged β- hairpin turn region are found to be mostly responsible for disturbing membrane. Even though the eventual membrane disruption requires Protegrin-1 oligomer, our simulations clearly show the first step of the monomeric effects. The thinning effects in the bilayer should relate to pore/channel formation in lipid bilayer and thus responsible for further defects in the membrane caused by oligomer. These results reveal first time how a peptide in β-hairpin conformation (rather than conventional α-helical structure) can disrupt membrane structure.

15. SUBJECT TERMS
Membrane-damaging, pore-forming, β-sheet, toxin, protegrin, antimicrobials, antibiotic

16. SECURITY CLASSIFICATION OF:			**17. LIMITATION OF ABSTRACT**	**18. NUMBER OF PAGES**	**19a. NAME OF RESPONSIBLE PERSON**
a. REPORT	**b. ABSTRACT**	**c. THIS PAGE**			USAMRMC
U	U	U	UU	31	**19b. TELEPHONE NUMBER** *(include area code)*

Table of Contents

Introduction

The Grant was proved in October 19, 2004 and the effective data started at October 25, 2008. The original research plan was scheduled to be finish in four year period from October 25, 2004 to October 24, 2008. Accordingly, we started our proposed research and recruit of postdoctoral researcher to fully concentrate at the project. The work to study the oligomerization of β-defensin and to study the protegrin-membrane interactions started immediately. We picked protegrin-1 as a model system to test our protocol to study the peptide dynamics, oligomerization, and membrane interactions. The postdoctoral researcher position at SAIC-Frederick was proved in December 2004. Dr. Jie Zheng was recruited in February 2005, to be started at June 2005. In May 18, 2005, we received notice that the program will be ended on Oct 24, 2006, which is two years ahead of initial research plan. We changed the work schedule accordingly, and Dr. Hyunbum Jang was hired to replace Jie Zheng in August 2005.

Despite of the unexpected change of program in the first year of the scheduled study, the proposed researches have been performed well during the first years of the project. Instead of starting all works (Bactenecins, Protegrin-1, β–Defensin, and C-terminal region of Phospholipases A_2) simultaneously, we have focused on two systems (Protegrin-1, β–Defensin) first. The major progresses have been made in PG-1 membrane interactions, and the β–defensin oligomerization also has preceded well. In a work related to the conformation search of C-terminal region of Phospholipases A_2), we tested a method to exhaustively search and rank conformational free energy with peptide size of C-terminal region of Phospholipases A_2. Based on the works conducted during the first of the research, the simulations of Bactenecins and C-terminal region of Phospholipases A_2 are planned to start at December, 2005.

Body

Current stage of β-defensin oligomerization.

Defensins are crucial to innate immunity. They contribute to the antimicrobial action of granulocytes, mucosal host defense in the small intestine and epithelial host defense in the skin and elsewhere (reviewed in [1]). The characteristic folds of defensins are β–sheets stabilized with three disulfide bonds. In humans there are three β–defensins: h β–defensin-1, -2 and -3, with similar sequences, however, different properties .

The main challenge for the activation mechanism of defense is the assembly in the membrane and the mechanism of membrane disruption. Our approaches are to evaluate the possible olgiomerization state of the β-defensin by multiple protein-protein docking method. We focus on two β-defensins, one is insect defensin Sapecin and another is human β-defensin-2 (HBD-2). The reason of choosing the two systems are: (1) We have experimental information about the possible protein-protein interactions and protein-membrane interactions for the insect defensin Sapecin[2]; and (2) Human β-defensin-2 (HBD-2) is biologically important due to its direct relationship with human, A understanding of mechanism is desired in order to design novel antimicrobial peptides that can be used as antibiotics to treat wounds, skins and systemic infections during military operations.

The current work on going is based on the following strategies (1) Firstly, we dock Sapecin using Symmdock to test the Sapecin trimeric assembly; and then we develop the scoring function for defensin assembly in membrane using experimental information as a guide. (2) Docking of HBD2 using symmdock to construct HBD2 octamers and using the optimized scoring function to

evaluate the HBD2 octamer in membrane. The flow chart of the computational approaches is reported here.

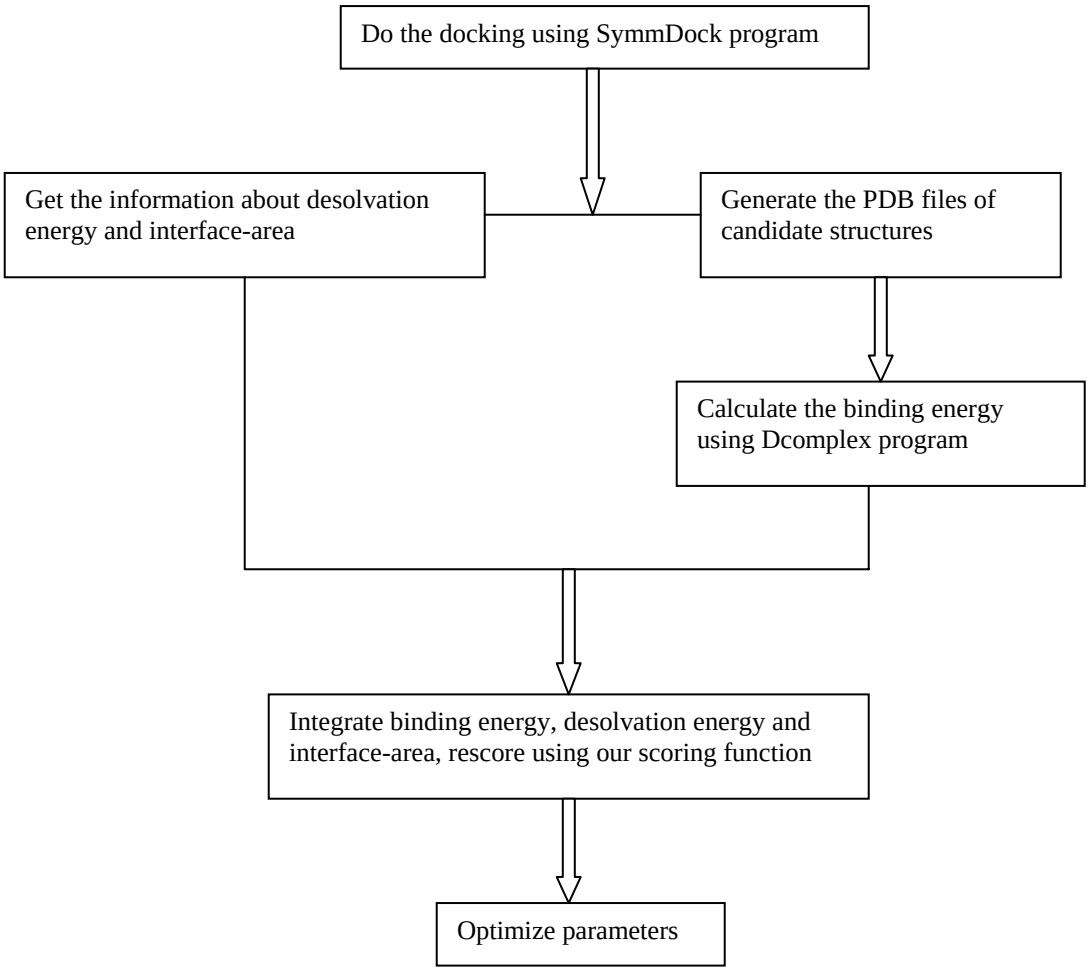

Figure 1. Flow chart for the strategy to investigate the defensin oligomerization in membrane.

The Symmdock is a program to dock protein oligomer in symmetric ways[3]. The Dcomplex is a program to calculate the protein-protein interaction using knowledge based functions[4]. Normal docking and scoring functions are designed for interaction in aqueous solution or in crystal complex. In order to reevaluate the docking solutions corresponding to membrane environment, we re-designed the scoring function used to rank the docked defensin oligomer as:

$\mathbf{E}_{membrane}$ = binding-energy*a + desolvation-energy*b + interface-area*c

Where the parameter a, b, and c are to be optimized from docking of Sapecin trimer in membrane. The binding energy is calculated with Dcomplex, and the desolvation energy and the interface area are calculated with the Symmdock. Based on extensive docking of the Sapecin and re-rank of the solution to fit experimental binding modes, we obtained the optimized parameters: a=1 , b = 0.006, and c=0.003.

NMR experiment has indicated the likely oligomer state for the Sapecin in membrane is [2]; :

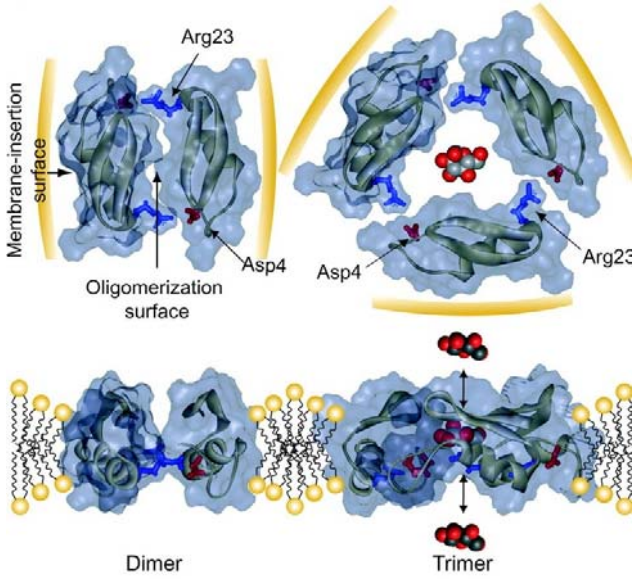

Figure 2. NMR suggested dimer and trimer of Sapecin with Salt bridging interactions (Asp4-Arg23).

In our study we limited our search to the Sapecin trimer, following the experimental suggestions illustrated in the Figure 2. We focus on the docking solutions with the important salt-bridge interactions. Our docking and rescoring has identified the two best solutions that have similar arrangement as the conformers suggested from experiment.

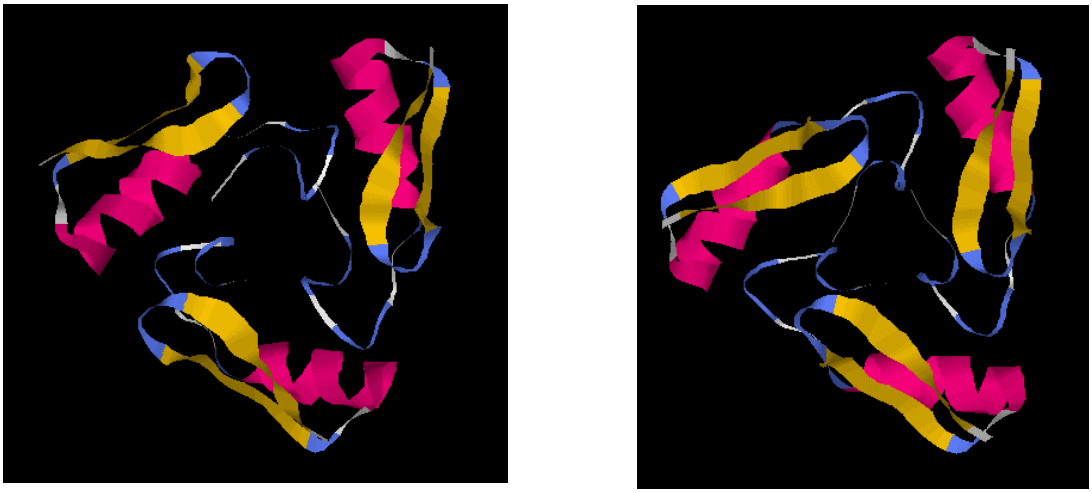

Figure 3. Two docked trimers identified to satisfy NMR suggested Salt bridging interactions (Asp4-Arg23).

In solution, the NMR structure for hBD2 does not show oligomerization. However, crystal structures of defensins indicate dimerization and oligomerization [5, 6]. A crystal packing pattern of human defensin might also provide information regarding pore formation in membrane. A pore formed by an octameric assembly could accommodate four water molecules[5]. The question is, though, if the assembly will re-arrange in the membrane. We try to use the parameters developed from docking of Sapecin to investigate the oligomerization of HBD2.

By apply the scoring functions developed from the Sapecin oligomer, we studied the oligomerization of hBD2. The new scoring function clearly helps to identify the possible channel forming oligomers in membrane. The twenty top ranking octamers have four structures with significant channel forming orientation.

Table 1. Top 20 ranked hBD2 octamers from symmdock with new scoring function. (The conformers with * are pore forming octamers)

rank	Score (new ranking)	Result (old ranking)
1	14.42336	result.103.pdb
2	13.41008	result.216.pdb
3	12.74822	result.172.pdb
4	12.48742	result.74.pdb
5*	12.48012	result.193.pdb
6	12.3413	result.97.pdb
7	12.02262	result.170.pdb
8	11.99962	result.251.pdb
9	11.91628	result.151.pdb
10	11.77326	result.133.pdb
11	11.53318	result.9.pdb
12*	11.4873	result.270.pdb
13	11.33686	result.175.pdb
14	11.27296	result.295.pdb
15	11.23988	result.429.pdb
16	11.14096	result.23.pdb
17	11.09774	result.255.pdb
18*	11.07944	result.87.pdb
19*	11.06372	result.124.pdb
20	10.91142	result.298.pdb

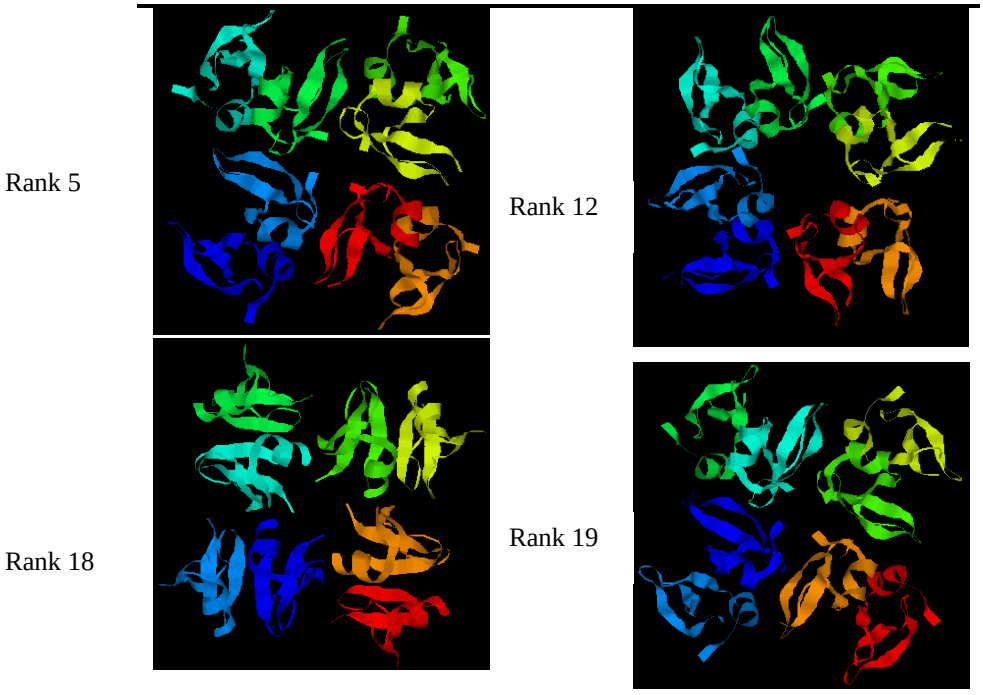

Figure 4. Four docked HBD2 octamers with pore forming confomation.

Currently, we are working on the two problems of the defensin oligomerization. (1) We are

trying to answer the question that if the Sapecin exist as dimer or trimer in membrane. Our initial work follows experimental suggestion that the trimer can explain the pore formation of the sapecin. Still, our current study indicates that more clasped state with small channel may be favorable for sapecin. Therefore, we think that it is necessary to examine the dimer as well. Even though a sapecin dimer can not form channel like conformation, the dimer may disrupt membrane to allow molecules passing through. Therefore, it is necessary to look further about sapecin membrane disruption mechanism. (2) We are also characterizing the pore forming HBD2 octamers identified from the docking study. We hope the further study can provide insights into the antimicrobial mechanism for human β-defensin. The work will be submitted for publication when we have the answers for the two questions discussed above.

Current stage of PG-1 oligomerization and membrane interaction.

Protegrin-1 enhances bacterial killing in thermally injured skin. Injuries from burning are common in the battlefield. PG-1 is particulary attractive for clinical use in human wounds since it retains a broad antimicrobial and antifungal activity at physiological salt concentration and in the presence of serum[7]. Protegrins have powerful antibiotic abilities but the molecular-level mechanisms underlying the interactions of their β-sheet motifs with the membrane are not known.

Protegrin-1 (PG-1) is composed of 18 amino-acid residues with a high content of basic residues and two disulfide bonds. We choose the PG-1 for our initial study and are planning to simulate Bactenecins to follow the protocols developed in the study of the PG-1. We started two directions of PG-1 simulations: (1) monomer conformations in solution and in membrane environment; and (2) dimer conformations in solution and membrane environment. Currently,

the dimer simulations are planned to be finished in the end of the year 2005, and the monomer-membrane interactions has been finished. The work has been submitted to the Journal of American Chemical Society and is under review process (see attached manuscript).

In the monomer simulations, we focused on the stability of PG-1 at the amphipathic interface in lipid bilayers and on the details of peptide-membrane interactions. We simulated all-atom models of the PG-1 monomer with explicit water and lipid bilayers composed of both homogeneous POPC lipids and a mixture of POPC:POPG (4:1) lipids. We observed that local thinning of lipid bilayers mediated by the peptide is enhanced in the lipid bilayer containing POPG, consistent with experimental results of selective membrane targeting. The β-hairpin motif of PG-1 is conserved in the both lipid setting, while it is highly bent in aqueous solution. The conformational dynamics of PG-1, especially the highly charged β-hairpin turn region are found to be mostly responsible for disturbing membrane. Even though the eventual membrane disruption requires PG-1 oligomer, our simulations clearly show the first step of the monomeric effects. The thinning effects in the bilayer should relate to pore/channel formation in lipid bilayer and thus responsible for further defects in the membrane caused by oligomer. These results reveal first time how a peptide in β-hairpin conformation (rather than conventional α-helical structure) can disrupt membrane structure.

Conformational Dynamics of Monomeric PG-1. We simulated PG-1, a β-hairpin peptide in different environments. In our simulations, the peptide, lipid bilayer, water, and salt are explicitly present in atomic detail. Experimentally, even though it is well-structured in solution, its structure cannot be resolved by NMR spectroscopy. However, the conformation is stabilized by the micelle environment, and a recent NMR study reveals its refined three-dimensional structure as consisting of a two-stranded antiparallel β-hairpin[8]. Our simulations

confirmed the conformational behaviors observed experimentally. Fig. 5 illustrates the simulated structures of PG-1 from the different envrionments. In the figure, the final structures of PG-1 are superimposed to show the conformational differences between the peptides from the pure bilayer system (red) and the mixed bilayer system (blue) with the NMR structure (gray). The upper and middle cartoons are the superimpositions from different views, and the lower cartoon is the final peptide conformation from the water box simulation. It can be clearly seen from the figure that the β-hairpin conformation is well retained in the presence of the lipid bilayers, although there is a slight conformational change from the NMR structure. In both lipid settings, the β-hairpins reorient the C-terminal β-strand, converting the overall β-hairpin to a cross β-sheet. The slightly bent β-strands found in the NMR structure become more elongated β-strands in the lipid setting.

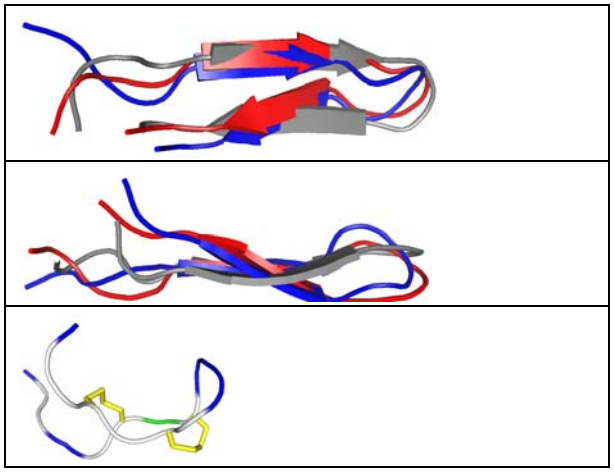

Figure 5. Superpositions of the final structures from the 10 *ns* simulations for PG-1 on the pure lipid bilayer composed of POPC (red) and on the mixed lipid bilayer composed of POPC:POPG (4:1) (blue) with the NMR structure (gray). The upper and middle cartoons are the same superpositions in different angle views, and the lower cartoon represents the final conformation of the peptide in the water box simulation (disulfide bonds are highlighted in yellow).

In the bulky water environment, PG-1 becomes a bent structure (lower Fig. 5). Nevertheless, the two disulfide bonds (yellow bonds, highlighted in the lower cartoon) hold the structure tightly; two strands locate closely near each other. The highly charged regions (turn and

terminals) are highly flexible in the aqueous solution, while the hydrophobic core is relatively stable. The hydrophobic core, reinforced by the two disulfide bonds, provided the nuclei for the peptide to refold back to the regular β-hairpin structure once it meets a proper environment. The conformational differences in aqueous solution and membrane environment suggest a great structural plasticity of the PG-1 β-hairpin mediated by the lipid bilayer.

The details of the conformational flexibility of the PG-1 are plotted with the root-mean-squared deviations (RMSD) relative to the starting point in Fig. 6 (averaged over the 10 *ns* simulations).

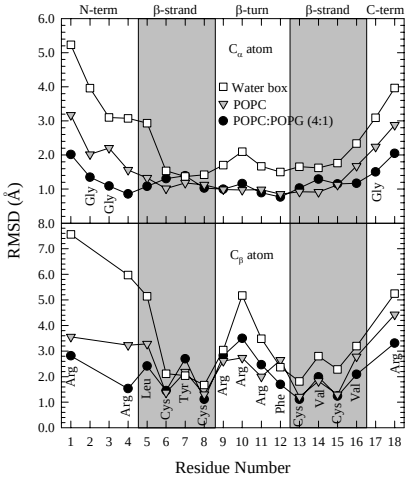

Figure 6. The average root-mean-squared deviation (RMSD) from the starting point for C_α atoms (upper) and C_β atoms (lower panel) of PG-1 in the water box (open squares), on the pure lipid bilayer composed of POPC (inverted gray triangles), and on the mixed lipid bilayer composed of POPC:POPG (4:1) (solid circles).

The figure shows the RMSDs of C_α atoms of the peptide backbone (upper) and C_β atoms of the side chains (lower panel) for PG-1 in the water box (open squares), and on the surfaces of pure lipid bilayer (inverted gray triangles) and mixed lipid bilayer (solid circles). PG-1 in the water environment shows higher mobility than on both lipid bilayers, especially for both N- and C-termini and β-turn regions. In contrast, PG-1 in both lipid settings has smaller deviation from the starting point, indicating that its average position stays close to the starting point. The active

motions of the Arg side chains in the β-turn are associated with the interactions of the peptide at the amphipathic interface with the lipid bilayer, and contribute to the membrane disruption effects of PG-1 (see results in next section).

Membrane Disturbing Effects by PG-1.

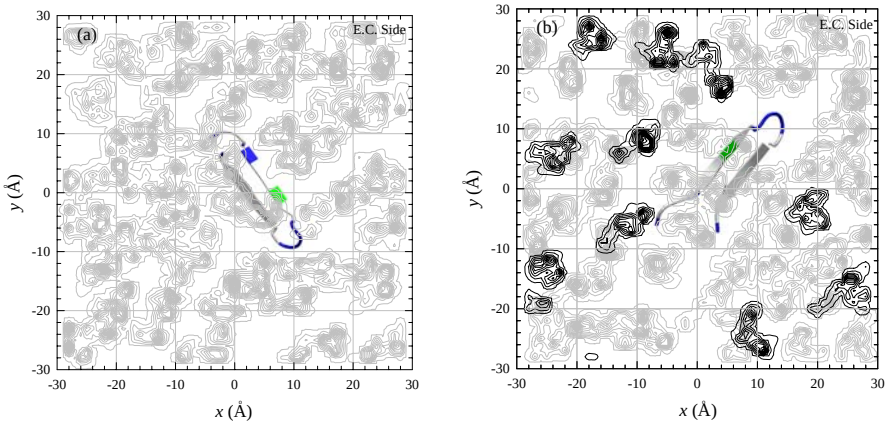

Figure 7. Mapping of *x*, *y* coordinates of the center of mass of each lipid on the extracellular half lipids onto the *x*-*y* plane for (a) the pure lipid bilayer composed of POPC and (b) the mixed lipid bilayer composed of POPC:POPG (4:1). The contour lines enclose highly populated locations of the center of mass of each POPC (gray lines) and POPG (black lines). The peptide is also projected onto the plane as an average structure with its average position during the simulation.

A striking effect of membrane disruption under the peptide invasion is revealed by analyzing the average position of lipid on the bilayer surface during the simulation. Fig. 8 shows the average positions of the center of mass of each of the extracellular half lipids on the *x*-*y* plane that can be defined as a projection of the bilayer surface. For the pure lipid bilayer system in Fig. 8(a), all lipids are distributed isotropically on the plane. On the other hand, for the mixed lipid bilayer system in Fig. 8(b), a significant deficiency in the distribution of the locations of the lipids' center of mass is evident from the wide empty space underneath the β-turn of PG-1. This is compelling evidence for the capability of PG-1 to disrupt/thin the membrane. The Arg residues in the β-turn stretch their long side chains parallel to the bilayer surface at the amphipathic

interface. The side chains interact strongly with the lipid heads located around the β-turn, in a way that the lipid heads tilt in the direction of the Arg side chain and the lipids' center of mass shifts to the end of the side chains. This leads to an absence of the lipids' center of mass around the β-turn. Consequently, the lipid bilayer exposes a hydrophobic bath to the peptide and the hydrophobic residue Phe, at the end of β-turn can easily immerse into this bath. Immersion of the hydrophobic side chain of Phe causes the conformational change of PG-1, in which the C-terminal β-strand is reoriented. We note that although the hydrophobic side chain immersion and the reorientation of the C- terminal β-strand are also monitored for PG-1 on the pure lipid bilayer, it is only on the mixed lipid bilayer that the peptide causes the local lipid integration/dissociation that is directly responsible for the bilayer thinning.

To further analyze the thinning effect mediated by PG-1, the three dimensional densities for the positions of the lipid headgroups are calculated during the 10 *ns* simulation. Fig. 8 shows the three dimensional density maps of the lipid headgroups for (a) the pure lipid bilayer and (b) the mixed lipid bilayers. In Figs. 8(a) and (b), the upper figure is a top view from the extracellular side with an embedded peptide, and the lower figure is a lateral view of the bilayer. The blue line in the lower figure connects the three mid points of the headgroup map, indicating the degree of the bilayer bending. The vertical double arrow in the lower figure points the degree of the bilayer thickness. The headgroup density map reflects the average shape of the bilayer surface during the simulation.

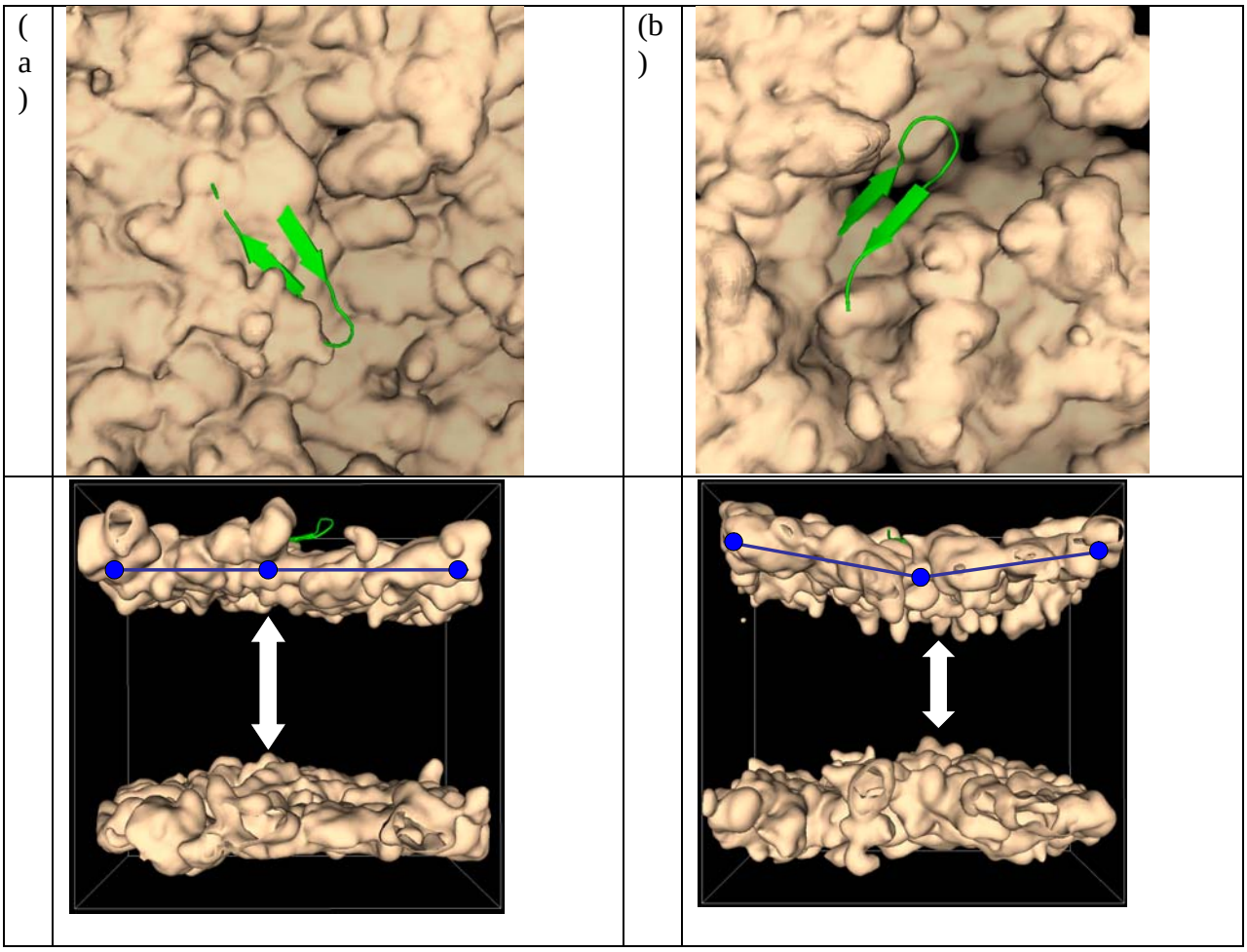

Figure 8. Three dimensional density maps of the lipid headgroup for (a) the pure lipid bilayer composed of POPC and (b) the mixed lipid bilayer composed of POPC:POPG (4:1). In both figures, the upper figure is the top view from the extracellular side with an embedded peptide, and the lower figure is the lateral view of the bilayer. In the lateral bilayer views, the blue lines are the three point connection that measures the bilayer bending, and the vertical double arrow points the degree of the bilayer thickness.

The pure lipid bilayer in Fig. 8(a) indicates some roughness of the bilayer surface. In the lateral view of the bilayer, the three point connection shows no symptom of a bending of the bilayer surface. For the mixed bilayer in Fig. 8(b), the roughness of bilayer surface becomes clearer. Furthermore, we observe that there is a dent or hole in the surface in the large area below the β-turn. The location of the dent in the bilayer surface is consistent with the location of the empty

space in Fig. 7(b). In the lateral view of the bilayer, the three point connection clearly indicates that there is significant bending of the extracellular surface. The bending of the bilayer surface is closely related with the membrane thinning effect. The vertical double arrow indicates a thinning of the bilayer. Compared with the pure lipid bilayer, the thickness of the mixed lipid bilayer is much smaller, particularly underneath the peptide.

Local thinning of the lipid bilayer due to the PG-1 invasion is clearer in the lipid bilayer with anionic lipids, which is consistent with an experimental observation[9]. The nature of the peptide conformational change and its function in a membrane environment, i.e. the anionic lipid setting, are keys to understanding the mechanism of the membrane thinning effect. Our simulation results provide important guidelines for how the environment supports the PG-1 conformation and how the PG-1 activity adapts to the environment. Recent experimental studies demonstrate that the solid-state aggregation of PG-1 is consistent with its ordered aggregatation in bilayers with the possible modes of intermolecular packing of PG-1 in the ordered aggregate[10, 11]. Further investigations of the PG-1 dimers in different intermolecular packing and in different settings of the lipid bilayers are being conducted to further our understanding of the complex behavior of membrane disruption.

Key Research Accomplishments

- Developed docking and scoring method for β-defensin oligomerization in membrane.
- Identified possible pore-forming oligomers of Human β-defensin-2.
- Characterized the conformational dynamics of Protegrin-1 in solution and in membrane.
- Revealed first time how a peptide in β-hairpin conformation (rather than conventional α-helical structure) can disrupt membrane structure.
- Studied the dimerization of Protegein-1 in solution and in membrane environment.
- Preliminary study of exhaustive conformation search of peptide with size of C-terminal region of Phospholipases A_2.

Reportable Outcomes

- One undergraduate student thesis by Mr. WenXun Gan, Department of Chemistry, Beijing University. 2005. Title:" Study of defensin's functional Native structure: A computational approach using protein-protein docking."
- One scientist is hired to simulate peptide-membrane interactions.
- One accepted manuscript to be published, related to peptide conformation search, stability, and oligomerization. "The stability of monomeric intermediates controls Amyloid formation: Aβ25-35 and its N27Q mutant". Buyong Ma and Ruth Nussinov, to be published on ***BioPhysical J.*** Manuscript abstract and acknowledgement attached.
- One manuscript under review, focused on cytolytic peptide-membrane interactions. Main achievement of the first year outcome. "Interaction of Protegrin-1 (PG-1) with Lipid Bilayers: Membrane Thinning Effect", Hyunbum Jang, Buyong Ma, Thomas Woolf, and Ruth Nussinov. **J. American Chemical Society.** Submitted. Manuscript attached.

Conclusions

We have mostly followed our initial plan described in the Statement of Work, with slightly adjustment of schedule. In the first year of research, we assembled the work force to carry out the proposed studies. Instead of starting all works (Bactenecins, Protegrin-1, β–Defensin, and C-terminal region of Phospholipases A_2) simultaneously, we have focused on two systems (Protegrin-1, β–Defensin) first. The major progresses have been made in PG-1 membrane interactions, and the β–defensin oligomerization also has preceded well. In a work related to the conformation search of C-terminal region of Phospholipases A_2, we tested a method to exhaustively search and rank conformational free energy with peptide size of C-terminal region of Phospholipases A_2. Based on the works conducted during the first of the research, the simulations of Bactenecins and C-terminal region of Phospholipases A_2) are planned to start at December, 2005.

The important scientific finding during the research period is the elucidation of peptide membrane thinning mechanism, detailed in the manuscript submitted to J. Amer. Chem. Soc. The effect is best illustrated by Figure 8 in this report. We observed that local thinning of lipid bilayers mediated by the peptide is enhanced in the lipid bilayer containing POPG, consistent with experimental results of selective membrane targeting. The conformational dynamics of PG-1, especially the highly charged β-hairpin turn region are found to be mostly responsible for disturbing membrane. Even though the eventual membrane disruption requires PG-1 oligomer, our simulations clearly show the first step of the monomeric effects. The thinning effects in the bilayer should relate to pore/channel formation in lipid bilayer and thus responsible for further defects in the membrane caused by oligomer. These results reveal first time how a peptide in β-hairpin conformation (rather than conventional α-helical structure) can disrupt membrane structure.

References

1. Ganz, T. Defensins: antimicrobial peptides of innate immunity. Nat Rev Immunol 3, 710-20 (2003).
2. Takeuchi, K. et al. Channel-forming membrane permeabilization by an antibacterial protein, sapecin: determination of membrane-buried and oligomerization surfaces by NMR. J Biol Chem 279, 4981-7 (2004).
3. Schneidman-Duhovny, D., Inbar, Y., Nussinov, R. & Wolfson, H. J. PatchDock and SymmDock: servers for rigid and symmetric docking. Nucleic Acids Res 33, W363-7 (2005).
4. Zhang, C., Liu, S., Zhu, Q. & Zhou, Y. A knowledge-based energy function for protein-ligand, protein-protein, and protein-DNA complexes. J Med Chem 48, 2325-35 (2005).
5. Hoover, D. M. et al. The structure of human beta-defensin-2 shows evidence of higher order oligomerization. J Biol Chem 275, 32911-8 (2000).
6. Hoover, D. M., Chertov, O. & Lubkowski, J. The structure of human beta-defensin-1: new insights into structural properties of beta-defensins. J Biol Chem 276, 39021-6 (2001).
7. Steinstraesser, L. et al. Protegrin-1 enhances bacterial killing in thermally injured skin. Crit Care Med 29, 1431-7 (2001).
8. Fahrner, R. L. et al. Solution structure of protegrin-1, a broad-spectrum antimicrobial peptide from porcine leukocytes. Chem Biol 3, 543-50 (1996).
9. Gidalevitz, D. et al. Interaction of antimicrobial peptide protegrin with biomembranes. Proc Natl Acad Sci U S A 100, 6302-7 (2003).
10. Tang, M., Waring, A. J. & Hong, M. Intermolecular packing and alignment in an ordered beta-hairpin antimicrobial peptide aggregate from 2D solid-state NMR. J Am Chem Soc 127, 13919-27 (2005).
11. Buffy, J. J., Waring, A. J. & Hong, M. Determination of peptide oligomerization in lipid bilayers using 19F spin diffusion NMR. J Am Chem Soc 127, 4477-83 (2005).

Appendices

1. Abstract and acknowledgement for the manuscript accepted by Biophysical J.
2. Manuscript of Protegrin-1 membrane interactions. “Interaction of Protegrin-1 (PG-1) with Lipid Bilayers: Membrane Thinning Effect”

1. Article accepted by Biophysical J.

The Stability of Monomeric Intermediates Controls Amyloid Formation: Aβ25-35 and its N27Q Mutant

Buyong Ma[1] and Ruth Nussinov [1,2]
[1] Basic Research Program, SAIC - Frederick, Inc.
Center for Cancer Research Nanobiology Program.
NCI-FCRDC, Frederick, MD 21702

[2] Sackler Inst. of Molecular Medicine
Department of Human Genetics and Molecular Medicine
Sackler School of Medicine
Tel Aviv University, Tel Aviv 69978, Israel

Keyword: Alzheimer's Disease, Amyloid, A-β peptide, intermediate, energy landscape, misfolding.

Correspondence and Requests for materials may be addressed to: Buyong Ma, mab@ncifcrf.gov; Ruth Nussinov, ruthn@ncifcrf.gov.

Abstract

The structure and stabilities of the intermediates affect protein folding as well as misfolding and amyloid formation. By applying Kramers' theory of barrier crossing and a Morse-function like energy landscape, we show that intermediates with medium stability dramatically increase the rate of amyloid formation; on the other hand, very stable and very unstable intermediates sharply decrease amyloid formation. Remarkably, extensive molecular dynamics simulations and conformational energy landscape analysis of Aβ25-35 and its N27Q mutant corroborate the mathematical description. Both experimental and current simulation results indicate that the core of the amyloid structure of Aβ25-35 formed from residues 28-35. A single mutation of N27Q of Aβ25-35 makes the Aβ25-35 N27Q amyloid free. Energy landscape calculations show that Aβ25-35 has extended intermediates with medium stability, which are prone to form amyloids, while the stability of extended intermediates for Aβ25-35 N27Q split into stable and very unstable species that are not disposed to form amyloids. The results explain the contribution of both α-helical as well as β-strand intermediates to amyloid formation. The results also indicate that the structure and stability of the intermediates, as well as of the native folded and the amyloid states can be targeted in drug design. One conceivable approach is to stabilize the intermediates to deter amyloid formation.

Acknowledgement

This project has been funded in whole or in part with Federal funds from the National Cancer Institute, National Institutes of Health, under contract number NO1-CO-12400 and by the US Army Medical Research Acquisition Activity under grant W81XWH-05-1-0002. Computations were conducted using the Biowulf cluster at the NIH, Bethesda, MD. The research of R. Nussinov in Israel has been supported in part by the *Center of Excellence in Geometric Computing and its Applications* funded by the Israel Science Foundation (administered by the *Israel Academy of Sciences*). The content of this publication does not necessarily reflect the views or policies of the Department of Health and Human Services, nor does mention of trade names, commercial products, or organizations imply endorsement by the U.S. Government. This research was supported (in part) by the Intramural Research Program of the NIH, National Cancer Institute, Center for Cancer Research.

Interaction of Protegrin-1 (PG-1) with Lipid Bilayers: Membrane Thinning Effect

Hyunbum Jang[1], Buyong Ma[1*], Thomas B. Woolf[2], and Ruth Nussinov[1,3]

[1]*Basic Research Program, SAIC-Frederick, Inc., Center for Cancer Research Nanobiology Program, NCI-FCRDC, Frederick, Maryland 21702,* [2]*Department of Physiology, Johns Hopkins University School of Medicine, Baltimore, Maryland 21205, and* [3]*Sackler Inst. of Molecular Medicine, Department of Human Genetics and Molecular Medicine, Sackler School of Medicine, Tel Aviv University, Tel Aviv 69978, Israel*

*Correspondence and Requests for materials may be addressed to: Buyong Ma, mab@ncifcrf.gov

Abstract: Protegrins, as cytolytic antimicrobial peptides, are thought be important in defending host tissues preventing infection via an attack on the membrane surface of invading microorganisms. Protegrins have powerful antibiotic abilities but the molecular-level mechanisms underlying the interactions of their β-sheet motifs with the membrane are not known. We focused on the stability of Protegrin-1 (PG-1) at the amphipathic interface with lipid bilayers and on the details of peptide-membrane interactions. PG-1, a β-hairpin peptide is composed of 18 amino-acid residues with a high content of cysteine and basic residues. It is further stabilized by two disulfide bonds between the cysteine residues. We simulated all-atom models of the PG-1 monomer with explicit water, salt, and lipid bilayers composed of both homogeneous POPC lipids and a mixture of POPC:POPG (4:1) lipids. We observed that the β-hairpin motif is conserved in both lipid environments. We further observed enhanced peptide-mediated local thinning of the lipid bilayers containing POPG. Even though the eventual membrane disruption requires PG-1 oligomer, our simulations clearly show the first step of the monomeric effects. The thinning effects are believed to be related to pore/channel formation in the lipid bilayer and thus responsible for the defects in the membrane.

Keywords: protegrin, membrane disruption, channel formation, dimerization, molecular dynamics simulations, antibiotic.

Introduction

Several hundreds of proteins/peptides are known to cause membrane damage and to lead to cell death. They are found in many organisms such as plants, insects, frogs, snakes and humans. Many such peptides are used by nature as either host defense (antimicrobial peptides) or offense (toxins from spider and snake venom). Since in these diseases the body produces peptides against its own cells, these disease-related peptides are involved in "autocytotoxic" conditions.[1] In addition to the wild cytolytic peptides, synthetic peptides modified from naturally occurring cytolytic peptides can also be cytotoxic, with mutation-sensitive activities.[2,3] The size of the protein ranges from a short peptide to several hundreds of amino-acids. Both large proteins and small peptides share a common feature, the ability to create a leakage pathway for molecules and ions to cross lipid bilayers.[4]

The monomeric structures of small cytolytic peptides can be classified into three groups: (1) α-helix, (2) β-sheet, and (3) loop strand. These peptides adopt totally different structures in different conditions, allowing the conformation to adjust to the surrounding environment. Most α-helical cytolytic peptides are largely random coil in solution and change to an α-helix within the membrane. The β-strand and loop strand peptides often have disulfide S-S bond(s) that constrain the peptide conformation.[5] Even though it is uncertain whether these disulfide bond-constrained peptides will have similar conformations in solution and in the membrane, it is commonly assumed that the disulfide bonds will keep the β-sheet structure unchanged. The most prominent characteristic of the small cytolytic peptides is that they are largely amphipathic, with hydrophobic and positively charged hydrophilic regions (with an excess of Lys and Arg residues). Positively charged residues can facilitate an initial contact between the peptides and the polyanionic sites in the membrane. Amphipathicity is essential for the membrane disruption effects by these peptides.[5]

One of the best characterized β-sheet cytolytic peptide is Protegrin. Native protegrins were originally purified from procine leukocytes, and there are five known porcine Protegrins, PG-1 to PG-5. These peptides share a common feature and conformation. Protegrin-1 (PG-1) forms the β-hairpin conformation, which is composed of 18 amino-acid residues (RGGRL-CYCRR-RFCVC-VGR) with a high content of cysteine (Cys) and positively charged arginine (Arg) residues, and is stabilized by two disulfide S-S bonds between the cysteine residues. The two disulfide bonds in PG-1 are crucial for the peptide activity, since the activity can be restored by stabilizing the peptide structure.[2] It was noted that the translocation ability of PG-1 is coupled to its pore-formation capacity and depends on its folding to the β-hairpin conformation.[6] As a representative β-sheet cytolytic peptide, PG-1 is a very potent antibiotic peptide.[7] Experimental NMR study has shown refined three-dimensional structure to consist of a two-stranded antiparallel β-hairpin in solution.[8]

The interaction of Protegrin with the membrane strongly depends on its lipid composition. Recent experimental studies have shown that PG-1 inserts readily into a membrane composed of negatively charged anionic lipids with the phosphatidylglycerol (PG) headgroup, but significantly less into a membrane composed of neutrally charged lipids with the phosphatidylcholine (PC) or phosphatidylethanolamine (PE) headgroups.[9] The major role of Protegrins in the membrane is a channel formation that causes an ion leakage. Recently, it has been reported that either PG-1 or PG-3 can induce weak anion-selective channels and potassium leakage from liposomes, and that PG-3 formed moderately cation-selective channels in the presence of bacterial lipopolysaccharide in planar phospholipid bilayers.[10] Formation of Protegrin channels disrupts the membrane surface by creating a pore across the membrane. Recent solid-state NMR indicates that PG-1 is fully immersed in the lipid bilayer and that a quantitative mismatch between the bilayer thickness and PG-1 length suggests a local thinning of the bilayer.[11,12] The

(1) Kourie, J. I.; Shorthouse, A. A. *Am. J. Physiol. Cell Physiol.* **2000**, 278, C1063-C1087.
(2) Lai, J. R.; Huck, B. R.; Weisblum, B.; Gellman, S. H. *Biochemistry* **2002**, 41, 12835-12842.
(3) Gobbo, M.; Biondi, L.; Filira, F.; Gennaro, R.; Benincasa, M.; Scolaro, B.; Rocchi, R. *J. Med. Chem.* **2002**, 45, 4494-4504.
(4) Panchal, R. G.; Smart, M. L.; Bowser, D. N.; Williams, D. A.; Petrou, S. *Curr Pharm Biotechnol.* **2002**, 3, 99-115.
(5) Sitaram, N.; Nagaraj, R. *Biochim. Biophys. Acta* **1999**, 1462, 29-54.
(6) Drin, G.; Temsamani, J. *Biochim. Biophys. Acta* **2002**, 1559, 160-170.
(7) Miyasaki, K. T.; Lehrer, R. I. *Int. J. Antimicrob. Agents* **1998**, 9, 269-280.
(8) Fahrner, R. L.; Dieckmann, T.; Harwig, S. SL.; Lehrer, R. I.; Eisenberg, D.; Feigon, J. *Chem. Biol.* **1996**, 3, 543-550.
(9) Gidalevitz, D.; Ishitsuka, Y.; Muresan, A. S.; Konovalov, O.; Waring, A. J.; Lehrer, R. I.; Lee, K. Y. *Proc. Natl. Acad. Sci. USA* **2003**, 100, 6302-6307.

thinning effect in the lipid bilayer is responsible for the formation of pore and/or channel in the membrane. PG-1 adopts a dimeric structure in DPC micelles, and a channel is formed by the association of several dimers.[13]

The molecular mechanisms of the membrane damage caused by non α-helical peptides are still unknown, and the structural basis for membrane disruption is not so apparent.[14] In this paper, we performed extensive molecular dynamics (MD) simulations of the PG-1 monomer in explicit water, salt, and lipid bilayers composed of both homogeneous POPC lipids and a mixture of POPC:POPG (4:1) lipids. MD simulations of the peptide conformational change and the membrane interactions can provide information complementary to experimental approaches. Our long term goal is to provide a detailed mechanism of the membrane disrupting effects by cationic peptides with β-sheet structure. We attempt, in this paper, to correlate the conformational change of the peptide and membrane thinning effects by PG-1. In aqueous solution, the PG-1 monomer becomes a more bent or collapsed structure with loss of β-sheet content. In contrast, the β-hairpin becomes more planar at the amphipathic interface with the lipid bilayer. The conformational change indicates that the bent β-hairpin structure can exert a "stress" force, pushing against the membrane surface. Here, we observe membrane thinning effects for the PG-1 monomer/anionic membrane system, consistent with experimental observations. Further investigation of the PG-1 oligomerization effects on the enhancement of the membrane thinning is underway. We believe that our current study provides insights into the first steps of the molecular mechanism of the membrane disrupting effects by the peptide.

Methods

The PG-1 structure obtained from NMR spectroscopy[8] (pdb numbers: 1PG1) was used for the all-atom simulations. The CHARMM program[15] and Charmm 27 force field were used to construct the set of starting points within an explicit environment (including lipid bilayers, water, and salts) and to relax the systems to a production-ready stage. For production runs, the NAMD code[16] on a Biowulf cluster[17] at the NIH was used for the starting point with the same Charmm 27 force field.

Building a Unit Cell Containing Lipid Bilayer. A unit cell that has two layers of lipids and contains almost 44,000 atoms is constructed. The β-hairpin structure of PG-1 used in the unit cell construction is the NMR structure. The peptide is initially located at the amphipathic region of the lipid bilayer on the extracellular side, with the two disulfide bonds facing the bilayer surface. The NMR structure was obtained in solution and does not provide any information regarding lipid molecules around the peptide. Our method closely follows a previous method, which has been successfully applied to gramicidin,[18] alpha helical systems,[19,20] rhodopsin,[21] bacteriorhodopsin,[22] and fusion domain of influenza hemagglutinin (HA).[23] Constant membrane surface area is maintained, with constant normal pressure applied in the direction perpendicular to the membrane to adequately maintain constant surface tension of the lipid bilayer throughout the simulation. The effective (time-averaged) surface tension is determined by choice of lateral cell dimensions.

Two different types of lipid bilayer are constructed for the simulations. One is a homogeneous (or pure) lipid bilayer containing a single type of lipid molecule, POPC (palmitoyl-oleyl-phosphatidylcholine). The other is a heterogeneous (or mixed) lipid bilayer containing a mixture of lipid molecules, POPC and POPG (palmitoyl-oleyl-phosphatidylglycerol) in a ratio of POPC:POPG (4:1). The cross-sectional areas per lipid for POPC and POPG are 63.5 $Å^2$ and 62.8 $Å^2$, respectively, as suggested by recent simulation studies.[24] With a choice for the number of lipid molecules, the optimal value of lateral cell dimensions can be determined. For the pure lipid bilayer, 100 POPCs (50 POPCs each side) constitute the lateral cell dimension of 56.35 Å × 56.35 Å. For the mixed lipid bilayer, 80 POPCs and 20 POPGs (40 POPCs and 10 POPGs each side) constitute the lateral cell dimension of 56.3 Å × 56.3 Å.

Simple vdW spheres representing lipid headgroups are placed in two parallel planes separated by the expected headgroup-to-headgroup lipid bilayer thickness, since the bilayer thickness is defined by the distance between the average positions of the phosphorus atoms in two mono layers. Recent simulation studies reported that the bilayer thickness is 35.5 Å for the pure POPC lipid bilayer and 36.0 Å for the pure POPG lipid bilayer at a temperature of 310 *K*.[24] We adopt a value of 35.5 Å for our POPC lipid bilayer and deduce a value of thickness of 35.6 Å for the mixed POPC:POPG (4:1) lipid bilayer. Dynamics is performed on the spheres, constrained to their respective planes. This planar harmonic constraint ensures that the vdW spheres are randomly distributed on the planes and is removed after the dynamics. The lipid bilayer is then constructed with headgroups at the positions of the vdW spheres. 100 lipid molecules were randomly selected from libraries (for each type of lipid) of pre-equilibrated liquid crystalline state lipids. After replacement of the vdW spheres with lipid molecules, the peptide is placed on the bilayer surface at the extracellular side. Rigid body dynamics, with constraints on the peptide backbone, was performed to obtain a better interfacial contact between the peptide and the lipid bilayer at the amphipathic interface.

A series of minimizations was performed to remove overlaps of the alkane chains and gradually relax the system. TIP3P waters were added and relaxed through a series of minimization and dynamics. Six counter ions (6 Cl^-) were inserted to electrically neutralize the pure lipid bilayer system, since there are six positively charged amino acid residues in the peptide. To obtain a physiological salt concentration near 100 *mM*, an additional 16 Na^+ and 16 Cl^- were added. The addition of explicit salt ions (more than charge-balancing counter ions) to near-physiological conditions is required for reducing artifacts on the peptide conformation during the simulations.[25,26] For the mixed lipid bilayer system, 14 Na^+ as counter ions are inserted to neutralize the system (the system contains 6 positively charged residues and 20 anionic lipids). 16 Na^+ and 16 Cl^- are also added to get the same salt concentration. The initial placement of the ions is located at the bulk water region, far from the peptide and the bilayer

(10) Sokolov, Y.; Mirzabekov, T.; Martin, D. W.; Lehrer, R. I.; Kagan, B. L. *Biochim. Biophys. Acta* **1999**, 1420, 23-29.
(11) Buffy, J. J.; Hong, T.; Yamaguchi, S.; Waring, A.J.; Lehrer, R. I.; Hong, M. *Biophys. J.* **2003**, 85, 2363-2373.
(12) Yamaguchi, S.; Hong, T.; Waring, A.; Lehrer, R. I.; Hong, M. *Biochemistry* **2002**, 41, 9852-9862.
(13) Roumestand, C.; Louis, V.; Aumelas, A.; Grassy, G.; Calas, B.; Chavanieu, A. *FEBS Lett.* **1998**, 421, 263-277.
(14) Bechinger, B. *Curr. Opin. Chem. Biol.* **2000**, 4, 639-644.
(15) Brooks, B. R.; Bruccoleri, R. E.; Olafson, B. D.; States, D. J.; Swaminathan, S.; Karplus, M. *J. Comput. Chem.* **1983**, 4, 187-217.
(16) Kalé, L.; Skeel, R.; Bhandarkar, M.; Brunner, R.; Gursoy, A.; Krawetz, N.; Phillips, J.; Shinozaki, A.; Varadarajan, K.; Schulten, K. *J. Comp. Phys.* **1999**, 151, 283-312.
(17) *This study utilized the high-performance computational capabilities of the Biowulf PC/Linux cluster at the National Institutes of Health, Bethesda, Md. (http://biowulf.nih.gov).*
(18) Woolf, T. B.; Roux, B. *Proc. Natl. Acad. Sci. USA* **1994**, 91, 11631-11635.
(19) Woolf, T. B. *Biophys. J.* **1997**, 73, 2376-2392.
(20) Woolf, T. B. *Biophys. J.* **1998**, 74, 115-131.
(21) Crozier, P. S.; Stevens, M. J.; Forrest, L. R.; Woolf, T. B. *J. Mol. Biol.* **2003**, 333, 493-514.
(22) Jang, H.; Crozier, P. S.; Stevens, M. J.; Woolf, T. B. *Biophys. J.* **2003**, 87, 129-145.
(23) Jang, H.; Michaud-Agrawal, N.; Woolf, T. B. **2005**, (to be submitted).
(24) Róg, T.; Murzyn, K.; Pasenkiewicz-Gierula, M. *Acta. Biochim. Polonica*. **2003**, 50, 789-798.
(25) Ibragimova, G. T.; Wade, R. C. *Biophys. J.* **1998**, 74, 2906-2911.
(26) Pfeiffer, S.; Fushman, D.; Cowburn, D. *Proteins* **1999**, 35, 206-217

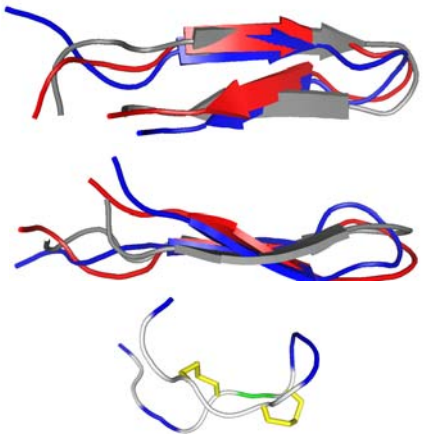

Figure 1. Superpositions of the final structures from the 10 *ns* simulations for PG-1 on the pure lipid bilayer composed of POPC (red) and on the mixed lipid bilayer composed of POPC:POPG (4:1) (blue) with the NMR structure (gray). The upper and middle cartoons are the same superpositions in different angle views, and the lower cartoon represents the final conformation of the peptide in the water box simulation (disulfide bonds are highlighted in yellow).

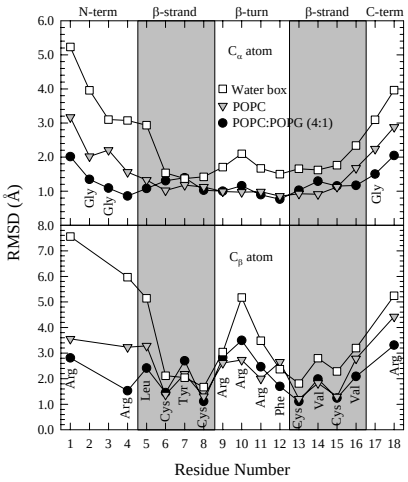

Figure 2. The average root-mean-squared deviation (RMSD) from the starting point for C_α atoms (upper) and C_β atoms (lower panel) of PG-1 in the water box (open squares), on the pure lipid bilayer composed of POPC (inverted gray triangles), and on the mixed lipid bilayer composed of POPC:POPG (4:1) (solid circles).

surfaces.[26] For two different lipid bilayer systems, many different initial configurations were constructed for the relaxation process. The simulation uses one of the best initial configurations as a starting point for the final production stage.

Building a Unit Cell for Water Box Simulation. Simulations without lipid molecules are relatively simple. A cubic water box with cell dimensions of 50 Å × 50 Å × 50 Å was constructed with the peptide held at the origin. The β-hairpin structure of PG-1 from the NMR is also used for the unit cell construction. Six counter ions (six Cl^-) were inserted to neutralize the system. In addition to the counter ions, six Na^+ and six additional Cl^- were also added to get a salt concentration near 100 *mM*. Salts were initially put far from the peptide. A series of minimization and dynamics for the solvent were performed with the peptide held rigid. The system was then ready for the relaxation process.

Relaxation of Initial Configurations and Production Runs. The initial configurations were gradually relaxed, with the peptide held rigid. In order to relax the solvent, dynamic cycles were performed with electrostatic cutoffs (12 Å) and constant temperature (Nosé-Hoover). This ensures that all degrees of freedom were adjusted as much as possible before the peptide starts to move. In subsequent stages, the peptide was harmonically restrained, with the harmonic restraints gradually diminishing, allowing the peptide to adjust to the surrounding solvent. Harmonic restraints on the peptide backbone atoms were gradually relaxed until gone, with the dynamics performed on the NPT ensemble. A Nosé-Hoover thermostat/barostat was used to maintain a constant temperature of 310 *K* for the lipid systems and 300 *K* for the water box and a constant pressure of 1 atm. Later equilibration stages include full Ewald electrostatics. Production runs of 10 ns for the starting points were performed on a Biowulf cluster[17] at the NIH. Analysis was performed with the CHARMM programming package.[15]

Results

Conformational Dynamics of Monomeric PG-1. We simulated PG-1, a β-hairpin peptide in different environments. In our simulations, the peptide, lipid bilayer, water, and salt are explicitly present in atomic detail. The β-hairpin of PG-1 consists of 18 amino acid residues with a high content of Cys and Arg residues and is stabilizedby two disulfide bonds between the Cys residues. Even with the two disulfide bonds, the monomeric PG-1 conformation is flexible. Experimentally, even though it is well-structured in solution,[6] its structure cannot be resolved by NMR spectroscopy. However, the conformation is stabilized by the micelle environment, and a recent NMR study reveals its refined three-dimensional structure as consisting of a two-stranded antiparallel β-hairpin.[8] Our simulations confirmed the conformational behaviors observed experimentally. Fig. 1 illustrates the simulated structures of PG-1 from the different envrionments. In the figure, the final structures of PG-1 are superimposed to show the conformational differences between the peptides from the pure bilayer system (red) and the mixed bilayer system (blue) with the NMR structure[8] (gray). The upper and middle cartoons are the superimpositions from different views, and the lower cartoon is the final peptide conformation from the water box simulation. It can be clearly seen from the figure that the β-hairpin conformation is well retained in the presence of the lipid bilayers, although there is a slight conformational change from the NMR structure. In both lipid settings, the β-hairpins reorient the C-terminal β-strand, converting the overall β-hairpin to a cross β-sheet. The slightly bent β-strands found in the NMR structure become more elongated β-strands in the lipid setting.

In the bulky water environment, PG-1 becomes a bent structure (lower Fig. 1). Nevertheless, the two disulfide bonds (yellow bonds, highlighted in the lower cartoon) hold the structure tightly; two strands locate closely near each other. The highly charged regions (turn and terminals) are highly flexible in the aqueous solution, while the hydrophobic core is relatively stable. The hydrophobic core, reinforced by the two disulfide bonds, provided the nuclei for the peptide to refold back to the regular β-hairpin structure once it meets a proper environment. The conformational differences in aqueous solution and membrane environment suggest a great structural plasticity of the PG-1 β-hairpin mediated by the lipid bilayer.

The details of the conformational flexibility of the PG-1 are plotted with the root-mean-squared deviations (RMSD) relative to the starting point in Fig. 2 (averaged over the 10 *ns* simulations). The figure shows the RMSDs of C_α atoms of the peptide backbone (upper) and C_β atoms of the side chains (lower panel) for PG-1 in the water box (open squares), and on the surfaces of pure lipid bilayer (inverted gray triangles) and mixed lipid bilayer (solid circles). The starting point used for reference is a relaxed structure in the CHARMM potential, with minor changes from the NMR structure.[8] Overall deviations that are very large (e.g., 5-10 Å or more) usually show an extremely flexible region. As expected, PG-1 in the water environment shows higher mobility than on both lipid bilayers, which is reflected in the larger deviation from the starting point, especially

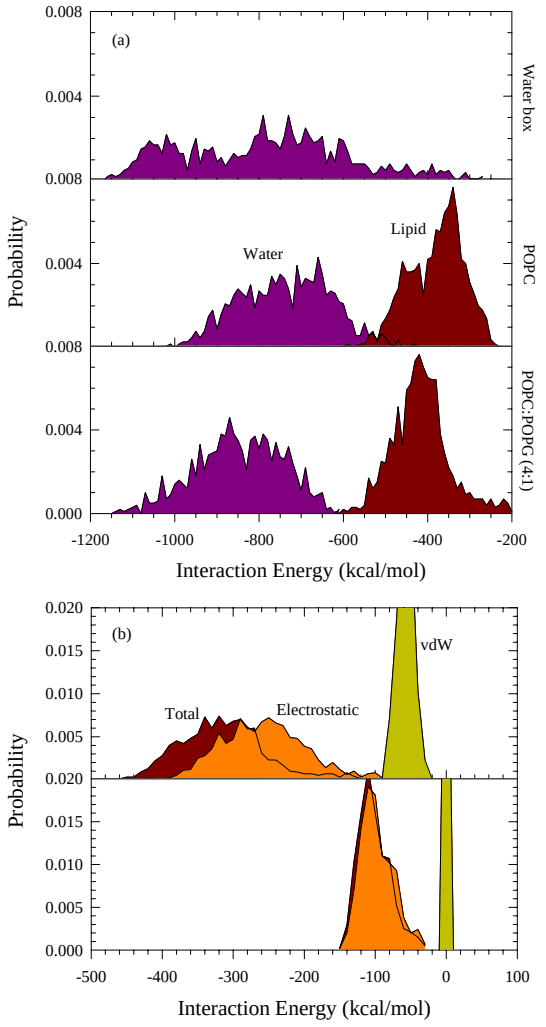

Figure 3. (a) Probability of interaction energies with the surrounding environments for PG-1 in the water box (upper), on the pure lipid bilayer composed of POPC (middle), and on the mixed lipid bilayer composed of POPC:POPG (4:1) (lower panel). (b) The interaction energy with the lipid is separated into POPC (upper) and POPG (lower) lipid parts for the mixed lipid bilayer system. The total interaction energies as well as the electrostatic contributions and the vdW contributions are shown.

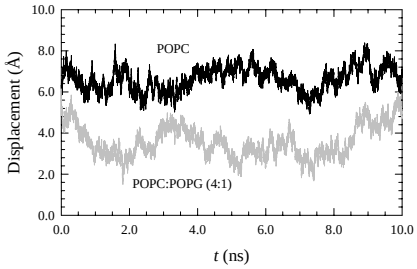

Figure 4. Time series of peptide displacement from the average position of phosphate atoms on the extracellular side for PG-1 on the pure lipid bilayer composed of POPC (black line) and the mixed lipid bilayer composed of POPC:POPG (4:1) (gray line).

for both N- and C-termini and β-turn regions. In contrast, PG-1 in both lipid settings has smaller deviation from the starting point, indicating that its average position stays close to the starting point. The larger fluctuations in the RMSD of the C_β atoms as compared to those of the C_α atoms reflects the larger motions of the side chains. Note, however, that there are significant motions in the Arg side chains of PG-1 in both lipid settings (residues 9 to 11) in the β-turn as compared to the corresponding backbone atoms. The active motions of the Arg side chains in the β-turn are associated with the interactions of the peptide at the amphipathic interface with the lipid bilayer, and contribute to the membrane disruption effects of PG-1 (see results in section C).

Energy Partition of Interaction between PG-1 and Lipids. The interaction energy between the peptide and the surrounding environment is calculated in order to understand the dominant forces that stabilize the β-hairpin structure. This is performed every 10 *ps* over the 10 *ns* simulations. Fig. 3(a) shows the resulting distributions of interaction energies for PG-1 in the water box (upper part of the figure), and for PG-1 on the surface of pure lipid bilayer (middle) and mixed lipid bilayer (lower). In the water box simulation, the interaction of PG-1 with water exhibits an isotropic behavior, since the distribution curve covers a wide range of interaction energies. However, in both lipid settings, the interactions of PG-1 with water and lipid exhibit distinct behavior, as indicated by the distribution peaks being located above specific interaction energy levels. The interactions of PG-1 with the surrounding environments share common features in both lipid settings, showing that PG-1 has stronger interactions with water than lipid, and the distribution curve for the interaction of PG-1 with lipid is much sharper. However, in contrast to these common features, PG-1 at the amphipathic interface in the mixed lipid bilayer has stronger interactions with both water and lipid than that in the pure lipid bilayer, as indicated by the locations of distributions peaks at lower energy levels.

To investigate the contributions of each type of lipid to the total interaction energy for the mixed bilayer system, the distribution of the peptide interaction energy with lipid is separated into POPC and POPG lipid parts. Fig. 3(b) shows the separated distributions of interaction energy with POPC (upper) and with POPG (lower) for PG-1 on the surface of the mixed lipid bilayer. The figure shows the total interaction energy distribution together with the electrostatic and vdW contributions. The total interaction of PG-1 with POPC is a sum of the electrostatic and vdW interactions, while the total interaction of PG-1 with POPG comes dominantly from the contribution of the electrostatic interaction. In fact, the distribution of the total peptide interaction energy with POPC in the mixed lipid bilayer is qualitatively similar to that with lipid in the pure lipid bilayer, since the pure lipid bilayer is also composed of POPC. By comparing the distribution of peptide interaction energies with POPC, a peak in the distribution curve is located at 320 kcal/mol for the mixed lipid bilayer system (as in the upper Fig. 3(b)), which is similar to the peak location at 340 kcal/mol for the pure lipid bilayer system (as in the middle of Fig. 3(a)). However, the interaction of PG-1 with lipid in the mixed lipid bilayer is much stronger than that in the pure lipid bilayer, since the peak in the distribution curve is located at 420 kcal/mol (the bottom panel of Fig. 3(a)). As seen in the lower part of Fig. 3(b), 100 kcal/mol (mainly electrostatic interactions) of the peptide interaction energy with the lipid in the mixed lipid bilayer system derive from the peptide interaction energy with POPG.

It can be expected that in the presence of anionic lipids, electrostatic interactions may be the dominant force in the peptide/membrane system. A favorable attraction between the PG-1 peptide containing 6 positively charged residues and the negatively charged bilayer surface might bring the peptide close to the bilayer surface. Thus, we investigate the peptide's location with respect to the bilayer surface. Fig. 4 shows the time series of the peptide's center of mass displacement from the bilayer surface for the pure lipid bilayer

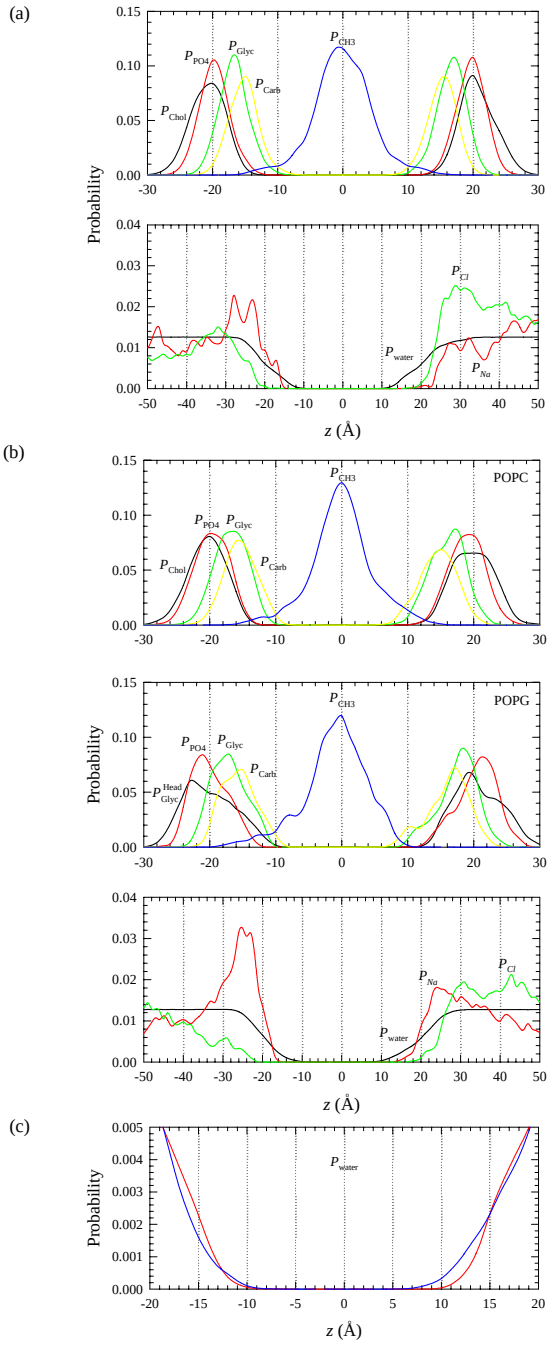

Figure 5. (a) Probability distribution functions (P) for different component groups of lipid (P_{Chol} (choline), P_{PO4} (phosphate), P_{Glyc} (glycerol), P_{Carb} (carbonyls), and P_{CH3} (methyl)) and for other solvents (P_{water} (water), P_{Na} (sodium ion), and P_{Cl} (chloride ion)) as a function of distance from the bilayer center for PG-1 on the pure lipid bilayer composed of POPC. (b) The same probability distribution functions for PG-1 on the mixed lipid bilayer composed of POPC:POPG (4:1). The probability distribution functions are separated into POPC (upper) and POPG (middle) lipid parts. In the distribution function for POPG, P_{Chol} (choline) from POPC is replaced by P^{Head}_{Glyc} (top-head glycerol). (c) Highlight of the probability distribution function for water, P_{water}, for the pure lipid bilayer (red) and for the mixed lipid bilayer systems (blue).

(black line) and the mixed lipid bilayer (gray line) systems. The bilayer surface is defined as the average position of the phosphate atoms on the extracellular side. As we expected, PG-1 on the surface of the mixed lipid bilayer is located closer to the bilayer surface than that on the pure lipid bilayer. This is consistent with the experimental observation that the ability of PG-1 to perturb and penetrate the anionic lipid bilayer is significantly enhanced compared to that of the zwitterionic lipid bilayer.[9] This suggests that the interaction of antimicrobial peptide PG-1 with the membrane strongly depends on the composition of lipid molecules in the membrane.

Membrane Disturbing Effects by PG-1. Lipids play important roles in supporting the conformation and dynamics of PG-1 at the amphipathic interface of the lipid bilayer. The average positions of lipid groups and other solvent molecules may provide useful information regarding the environmental response to the peptide dynamics during the simulation. Fig. 5(a) shows the position probability distribution functions (P) for five different component groups of POPC (upper), water, and salts (lower) as a function of the distance from the pure POPC lipid bilayer center. The POPC headgroup is divided into four subunits, choline (P_{Chol}, black line), phosphate (P_{PO4}, red line), glycerol (P_{Glyc}, green line), and carbonyl (P_{Carb}, yellow line). The tail group involves two fatty acids with terminal methyl (P_{CH3}, blue line). The peptide is located at the amphipathic region of the lipid bilayer on the extracellular side

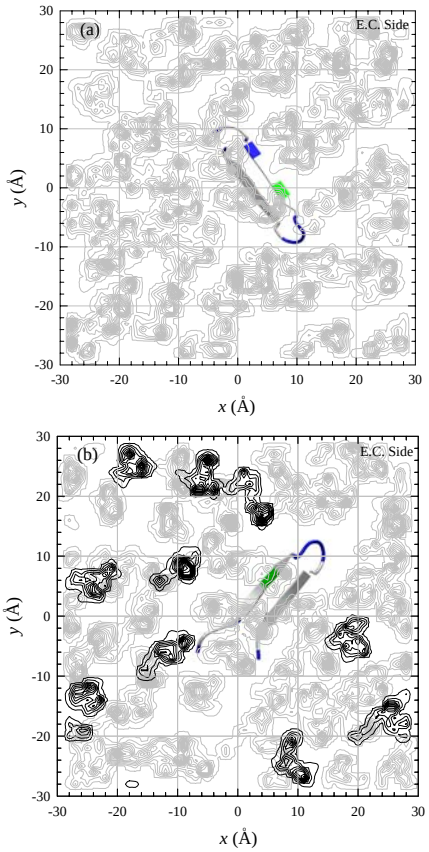

Figure 6. Mapping of x, y coordinates of the center of mass of each lipid on the extracellular half lipids onto the x-y plane for (a) the pure lipid bilayer composed of POPC and (b) the mixed lipid bilayer composed of POPC:POPG (4:1). The contour lines enclose highly populated locations of the center of mass of each POPC (gray lines) and POPG (black lines). The peptide is also projected onto the plane as an average structure with its average position during the simulation.

(a) (b)

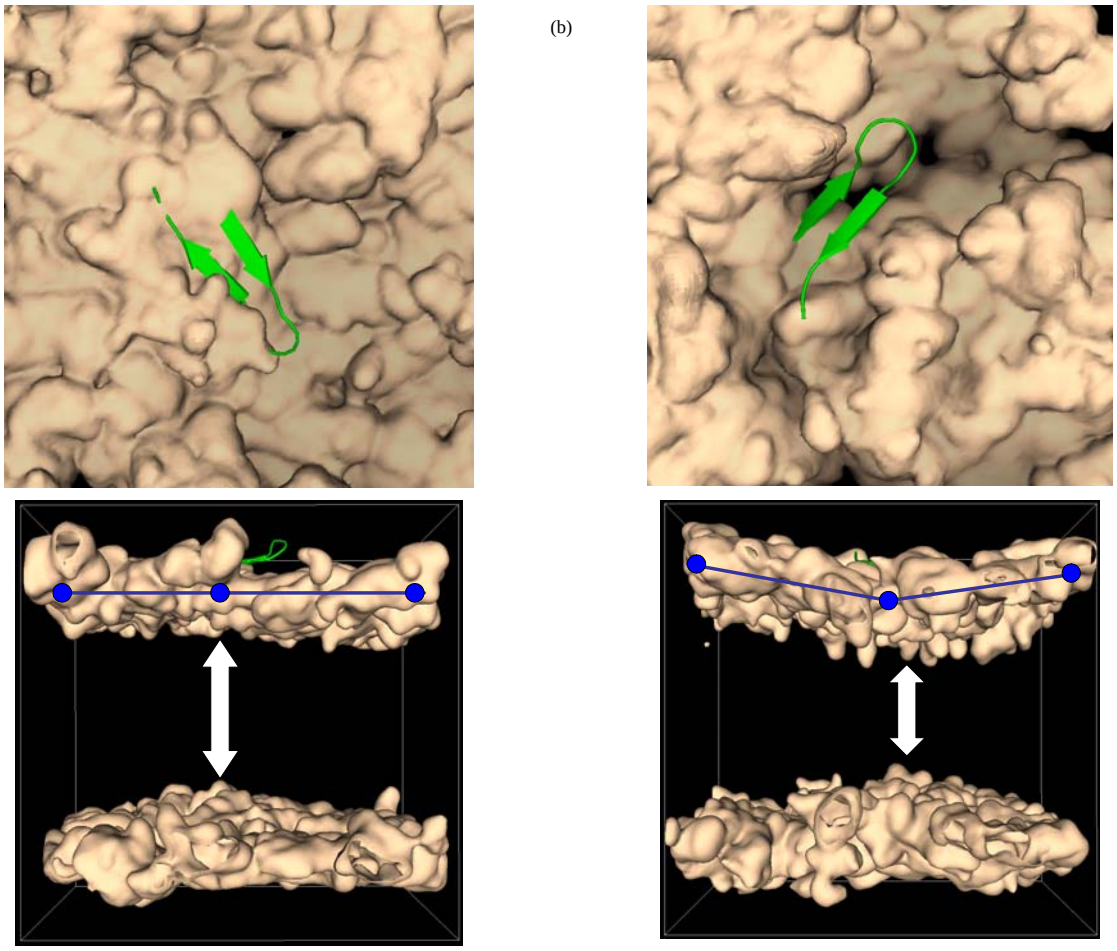

Figure 7. Three dimensional density maps of the lipid headgroup for (a) the pure lipid bilayer composed of POPC and (b) the mixed lipid bilayer composed of POPC:POPG (4:1). In both figures, the upper figure is the top view from the extracellular side with an embedded peptide, and the lower figure is the lateral view of the bilayer. In the lateral bilayer views, the blue lines are the three point connection that measures the bilayer bending, and the vertical double arrow points the degree of the bilayer thickness.

(positive *z* area), while the intracellular side (negative *z* area) contains lipids only. For the pure lipid bilayer system, symmetric behavior in the distributions of the lipid headgroups indicates that there is less disturbance in the lipid arrangement from the peptide. But, a small degree of disorder in the lipid tails is monitored as indicated by a plateau located at z = 4 Å in the P_{CH3} curve. In the distributions of salts, the probability for finding sodium ions near the bilayer surface at the intracellular side is high, while at the extracellular side a large number of chloride ions accumulate in the region next to the peptide.

The same position probability distribution functions (P) for the mixed lipid bilayer composed of POPC:POPG (4:1) is calculated by collecting data separated into POPC and POPG parts. Fig. 5(b) shows position probability distribution functions (P) for five different component groups of POPC (upper) and POPG (middle), water, and salts (lower) as a function of the distance from the bilayer center for the mixed lipid. In POPG, a glycerol (P_{Glyc}^{Head}) subunit at the top of the lipid head replaces the choline subunit present in POPC. The peptide induces an asymmetry in the distribution of POPC headgroups. It can be seen that the POPC headgroups on the extracellular side are distributed along the membrane normal more widely than those on the intracellular side. In the distribution of POPG headgroups, disordered arrangements of POPG heads are observed on both sides of the bilayer. Although not shown in the figure, we observed lipids with significantly disordered tails, especially for lipids in contact with the peptide. We suspect that the disordering of lipid tails causes the thinning of the lipid bilayer. In the distribution of salts, compared to the pure bilayer system, the probability of sodium ions near the bilayer surface at the intracellular side is very high due to the strong electrostatic attraction between sodium ions and the anionic lipids in the bilayer. On the extracellular side, the probability of sodium ions is smaller, indicating that the presence of the peptide on the bilayer surface reduces the sodium attraction. Chloride ions at the extracellular side are repelled from the bilayer surface, since the peptide/bilayer system still has a net negative charge.

Water molecules in the mixed lipid bilayer behave differently compared to those in the pure lipid bilayer. In Fig. 5(c), the position probability distribution function for water, P_{water}, is highlighted in order to compare the differences between the pure lipid bilayer (red) and the mixed lipid bilayer (blue) systems. On the intracellular side, the probability curves for water reduce to zero at z = -9 Å for both bilayer systems. However, on the extracellular side more water molecules penetrate into the hydrophobic region in the mixed lipid bilayer. The large number of water molecules penetrating the mixed

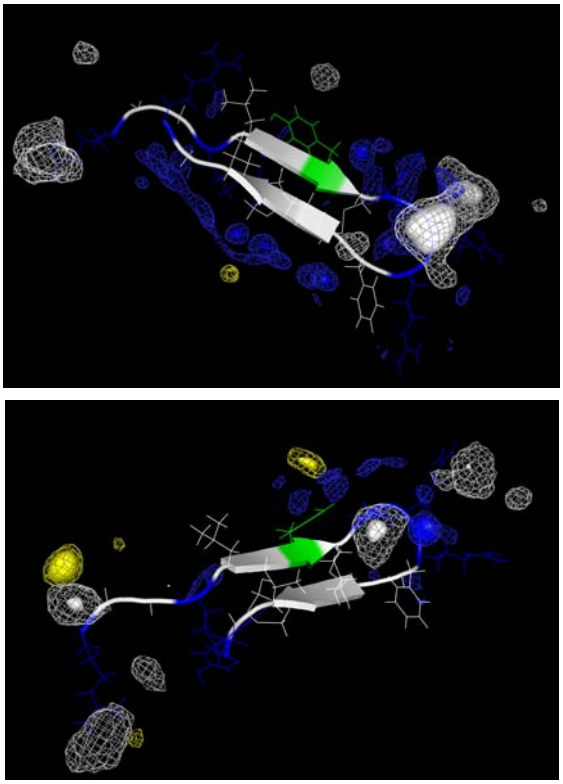

Figure 8. Three dimensional density map of water (blue), sodium (yellow), and chloride (white) ions for the pure lipid bilayer composed of POPC (upper) and the mixed lipid bilayer composed of POPC:POPG (4:1) (lower).

lipid bilayer can characterize the complex amphipathic dynamics between the peptide and the lipid bilayer and the thinning pathway.

A striking effect of membrane disruption under the peptide invasion is revealed by analyzing the average position of lipid on the bilayer surface during the simulation. Fig. 6 shows the average positions of the center of mass of each of the extracellular half lipids on the *x-y* plane that can be defined as a projection of the bilayer surface. The contour lines enclose highly populated center of mass positions of each POPC (gray lines) and POPG (black lines) on the extracellular side. The peptide is also projected onto the plane as an average structure with its average position during the simulation. For the pure lipid bilayer system in Fig. 6(a), all lipids are distributed isotropically on the plane. On the other hand, for the mixed lipid bilayer system in Fig. 6(b), a significant deficiency in the distribution of the locations of the lipids' center of mass is evident from the wide empty space underneath the β-turn of PG-1. This is compelling evidence for the capability of PG-1 to disrupt/thin the membrane. The Arg residues in the β-turn stretch their long side chains parallel to the bilayer surface at the amphipathic interface. The side chains interact strongly with the lipid heads located around the β-turn, in a way that the lipid heads tilt in the direction of the Arg side chain and the lipids' center of mass shifts to the end of the side chains. This leads to an absence of the lipids' center of mass around the β-turn. Consequently, the lipid bilayer exposes a hydrophobic bath to the peptide and the hydrophobic residue Phe, at the end of β-turn can easily immerse into this bath. Immersion of the hydrophobic side chain of Phe causes the conformational change of PG-1 shown in Fig. 1, in which the C-terminal β-strand is reoriented. We note that although the hydrophobic side chain immersion and the reorientation of the C-terminal β-strand are also monitored for PG-1 on the pure lipid bilayer, it is only on the mixed lipid bilayer that the peptide causes the local lipid integration/dissociation that is directly responsible for the bilayer thinning.

To further analyze the thinning effect mediated by PG-1, the three dimensional densities for the positions of the lipid headgroups are calculated during the 10 *ns* simulation. Fig. 7 shows the three dimensional density maps of the lipid headgroups for (a) the pure lipid bilayer and (b) the mixed lipid bilayers. In Figs. 7(a) and (b), the upper figure is a top view from the extracellular side with an embedded peptide, and the lower figure is a lateral view of the bilayer. The blue line in the lower figure connects the three mid points of the headgroup map, indicating the degree of the bilayer bending. The vertical double arrow in the lower figure points the degree of the bilayer thickness. The headgroup density map reflects the average shape of the bilayer surface during the simulation. The pure lipid bilayer in Fig. 7(a) indicates some roughness of the bilayer surface. In the lateral view of the bilayer, the three point connection shows no symptom of a bending of the bilayer surface. For the mixed bilayer in Fig. 7(b), the roughness of bilayer surface becomes clearer. Furthermore, we observe that there is a dent or hole in the surface in the large area below the β-turn. The location of the dent in the bilayer surface is consistent with the location of the empty space in Fig. 6(b). In the lateral view of the bilayer, the three point connection clearly indicates that there is significant bending of the extracellular surface. The bending of the bilayer surface is closely related with the membrane thinning effect. The vertical double arrow indicates a thinning of the bilayer. Compared with the pure lipid bilayer, the thickness of the mixed lipid bilayer is much smaller, particularly underneath the peptide.

The density map calculations also give us useful information on the exact interaction sites around the peptide by the solvent including water and ions. Fig. 8 shows the density maps of water (blue), sodium (yellow), and chloride (white) ions for PG-1 on the pure lipid bilayer (upper) and the mixed lipid bilayer (lower panel). The average structures of the peptide during the 10 *ns* simulation are presented in the figure with color codes as following: blue-positively charged residue, white-hydrophobic, and green-polar residue. An isomesh encloses the same probability values in space, and an isosurface encloses higher probability values than the isomesh. For PG-1 on the pure bilayer, water solvation sites with probabilities of 0.4/0.5 (mesh/surface) are observed around the peptide. Popular chloride interaction sites with probabilities of 0.02/0.03 (mesh/surface) around the β-turn indicate that the Arg side chains have strong electrostatic interactions with chloride ions. Sodium interaction sites with probabilities of 0.01 (mesh) are relatively rare. For PG-1 on the mixed bilayer, water solvation sites with probabilities of 0.4/0.5 (mesh/surface), chloride interaction sites with probabilities of 0.015/0.02 (mesh/surface), sodium interaction sites with probabilities of 0.015/0.02 (mesh/surface) are observed. Compared with the pure bilayer system, chloride interaction sites around the β-turn are reduced in the mixed bilayer system. Here, the chloride ions are repelled from the bilayer surface due to the negative nature of the lipid interface/peptide system. This suggests that the Arg side chains interact more with lipid molecules in the mixed bilayer. In other words, the interactions of the Arg side chains with lipid molecules in the pure bilayer system are screened by chloride ions. This can explain partly the fact that PG-1 interaction with the lipid bilayer is enhanced in the presence of negatively charged lipids in the membrane.

Discussion

We simulated the Protegrin-1 (PG-1) monomer in different environments: an explicit water box containing salts, pure lipid bilayer composed of POPC, and a mixed lipid bilayer composed of POPC:POPG (4:1). In our simulations, the bulk water environment

does not support the β-hairpin structure of PG-1 that was defined from NMR spectroscopy.[8] However, in both lipid bilayer settings the β-hairpin structure of PG-1 is well preserved. In addition, PG-1 adapts to the new lipid-rich environments through a structural rearrangement in the C-terminal β-strand. Importantly, the new PG-1 conformation at the amphipathic interface with the lipid bilayer implies that PG-1 is ready to conduct its physiological activity in the membrane. PG-1 is known as a membrane damaging peptide with a great antibiotic potentcy.[7] The PG-1 activity is strongly supported by its stable β-hairpin conformation.[2] Although PG-1 loses its β-hairpin motif in a bulk water environment, the two disulfide S-S bonds in PG-1 hold the structure tightly, and the β-hairpin can be easily refolded in a proper environment. This large conformational plasticity of PG-1 due to the disulfide bonds is mediated by the amphipathic interface at the lipid bilayer.

The detailed mechanisms of the membrane disruption, especially those caused by β-sheet peptides, are still unclear.[14] In this paper, our attention focuses on the conformational change of PG-1 at the amphipathic interface of the lipid bilayer and on the bilayer thinning by the peptide. PG-1 shares a common conformation at the amphipathic interface of the bilayer, and the structure differs from the solution NMR structure.[8] However, PG-1 exhibits different features at the interface of lipid bilayers with different lipid compositions. In the presence of anionic lipids in the bilayer, PG-1 locates more closely to the bilayer surface and interacts more strongly with the lipids, although the peptide has the same initial height from the bilayer surface in the starting points for both lipid bilayers. Local thinning of the lipid bilayer due to the PG-1 invasion is clearer in the lipid bilayer with anionic lipids, which is consistent with an experimental observation.[9] The nature of the peptide conformational change and its function in a membrane environment, i.e. the anionic lipid setting, are keys to understanding the mechanism of the membrane thinning effect. Our simulation results provide important guidelines for how the environment supports the PG-1 conformation and how the PG-1 activity adapts to the environment. We suggest that the membrane disrupting effects such as pore/channel formation are directly mediated by packing of PG-1 dimers into ordered aggregates.[13,27,28] Recent experimental studies demonstrate that the solid-state aggregation of PG-1 is consistent with its ordered aggregatation in bilayers with the possible modes of intermolecular packing of PG-1 in the ordered aggregate.[27,28] Further investigations of the PG-1 dimers in different intermolecular packing and in different settings of the lipid bilayers are being conducted to further our understanding of the complex behavior of membrane disruption.

(27) Buffy, J. J.; Waring A. J.; Hong, M. *J. Am. Chem. Soc.* **2005**, 127, 4477-4483.
(28) Tang, M.; Waring, A. J.; Hong, M. *J. Am. Chem. Soc.* **2005**, 127, 13919-13927.

Acknowledgment. This project has been funded in whole or in part by the US Army Medical Research Acquisition Activity under grant W81XWH-05-1-0002 and with Federal funds from the National Cancer Institute, National Institutes of Health, under contract number NO1-CO-12400. The content of this publication does not necessarily reflect the views or policies of the Department of Health and Human Services, nor does mention of trade names, commercial products, or organizations imply endorsement by the U.S. Government. This research was supported (in part) by the Intramural Research Program of the NIH, National Cancer Institute, Center for Cancer Research. This study utilized the high-performance computational capabilities of the Biowulf PC/Linux cluster at the National Institutes of Health, Bethesda, MD (http://biowulf.nih.gov).